CBCT-Based Adaptive Assessment Workflow for Intensity Modulated Proton Therapy for Head and Neck Cancer

Mariluz De Ornelas, PhD; Yihang Xu, MS; Kyle Padgett, PhD; Ryder M. Schmidt, MS; Michael Butkus, PhD; Tejan Diwanji, MD; Gus Luciani; Jason Lambiase; Stuart Samuels, MD, PhD; Michael Samuels, MD; Nesrin Dogan, PhD

Department of Radiation Oncology, University of Miami Miller School of Medicine, Miami, FL, USA

Abstract

Purpose: Anatomical changes and patient setup uncertainties during intensity modulated proton therapy (IMPT) of head and neck (HN) cancers demand frequent evaluation of delivered dose. This work investigated a cone-beam computed tomography (CBCT) and deformable image registration based therapy workflow to demonstrate the feasibility of proton dose calculation on synthetic computed tomography (sCT) for adaptive IMPT treatment of HN cancer.

Materials and Methods: Twenty-one patients with HN cancer were enrolled in this study, a retrospective institutional review board protocol. They had previously been treated with volumetric modulated arc therapy and had daily iterative CBCT. For each patient, robust optimization (RO) IMPT plans were generated using ±3 mm patient setup and ±3% proton range uncertainties. The sCTs were created and the weekly delivered dose was recalculated using an adaptive dose accumulation workflow in which the planning computed tomography (CT) was deformably registered to CBCTs and Hounsfield units transferred from the planning CT. Accumulated doses from ±3 mm/±3% RO-IMPT plans were evaluated using clinical dose-volume constraints for targets (clinical target volume, or CTV) and organs at risk.

Results: Evaluation of weekly recalculated dose on sCTs showed that most of the patient plans maintained target dose coverage. The primary CTV remained covered by the V95 > 95% (95% of the volume receiving more than 95% of the prescription dose) worst-case scenario for 84.5% of the weekly fractions. The oral cavity accumulated mean dose remained lower than the worst-case scenario for all patients. Parotid accumulated mean dose remained within the uncertainty bands for 18 of the 21 patients, and all were kept lower than RO-IMPT worst-case scenario for 88.7% and 84.5% for left and right parotids, respectively.

Conclusion: This study demonstrated that RO-IMPT plans account for most setup and anatomical uncertainties, except for large weight-loss changes that need to be tracked throughout the treatment course. We showed that sCTs could be a powerful decision tool for adaptation of these cases in order to reduce workload when using repeat CTs.

Keywords: dose accumulation; IMPT; head and neck cancer

Introduction

Radiotherapy for head and neck (HN) cancer is used as a primary treatment or as an adjuvant to surgery to achieve tumor control and limit toxicity to nearby organs at risk (OARs). It is therefore imperative that the delivery of radiotherapy is both accurate and precise. The complex anatomy in the HN region has made intensity modulated radiation therapy (IMRT) the treatment of choice because of its ability to create highly conformal treatment plans in treatment sites with complex target geometry where many OARs are proximal to the targets. However, IMRT in patients with substantial target volume changes or significant weight loss can be challenging and may result in underdosage of targets and overdosage of OARs [1–3]. It has been well documented that significant anatomical changes are common during HN treatment courses, which may require plan adaptation to maintain optimal target coverage and continued sparing of OARs. Adaptive radiotherapy (ART) in the HN setting typically requires the patient to be re-scanned and replanned during the treatment course in order to accommodate for these changes. However, ART is time consuming and resource intensive; therefore, the clinician's judgment plays an important role in determining the need for adaptation [3, 4].

Intensity modulated proton therapy (IMPT) is well suited to HN treatments and can achieve steep dose gradients, which results in better sparing of OARs compared with IMRT [1]. However, the benefits of IMPT come at a cost of increased uncertainties in dose delivery compared with IMRT. These uncertainties include setup errors, anatomical changes, and proton beam range uncertainties [2, 3], and they can become compounded in situations in which there are significant target volume changes or significant weight loss. Imperfect daily alignments and anatomical changes may introduce large dose variations due to the sharp dose gradients at the end of the proton range; these uncertainties are increased when the proton beam encounters various tissue types (tissue, bone, and air). This sensitivity to changes can make the delivered dose in proton therapy deviate significantly from the planned proton dose compared with conventional IMRT. Therefore, it is important to quantify the dosimetric impact of anatomical changes and patient setup uncertainties during proton therapy of HN cancers.

To help mitigate uncertainties in proton planning, robust optimization (RO), accounting for both setup and range uncertainties, has become standard in IMPT planning, eliminating the need for a target expansion [4]. Since anatomical changes are patient dependent, and proton therapy is more sensitive to changes in anatomy, such changes need to be assessed more frequently during the treatment course to determine the need for ART compared with photon treatments. In many HN ART strategies, the difference between the planned and the delivered dose is estimated by calculating the dose distribution on repeated computed tomography (rCT) scans and reoptimizing the plan if a significant deviation is detected [5]. Daily image guided radiation therapy using online cone beam computed tomography (CBCT) provides tracking of daily positioning and anatomical changes of patients in treatment positions. It has the potential to be used to evaluate dose rather than using rCT scans, which involve more resources and time, as well as increasing imaging dose to a patient. However, the use of CBCTs for proton dose calculations is challenging due to increased scatter, motion, beam hardening, Hounsfield unit (HU) inaccuracy, and often smaller field of view (FOV) sizes. Some studies have shown that by applying a scatter correction algorithm and calculating the water equivalent path length dosimetric calculations can be performed on CBCT scans [6–8].

Previous studies have used synthetic computed tomography (sCT) for proton dose calculations [8–12]. These sCTs are obtained by deforming planning computed tomography (pCT) images into the daily CBCT frame of reference and subsequently transferring the pCT HUs to obtain the corresponding stopping power maps for calculating dose. Kurz et al [9] demonstrated that sCT adapted plans were similar to the original plan and yielded lower maximum dose values for the target compared with rCT adapted plans. Another study performed gamma index evaluation and dose volume histogram (DVH) statistics and found that the sCT dose distributions agreed well with those on the rCT [10]. A study by van de Water et al [11] generated sCTs with varying nasal cavity filling and demonstrated that RO plans can effectively deal with such variations throughout the treatment course for patients with sinonasal tumors, yet demonstrated higher OAR doses compared to rCT plan adaptation. More recently, Hague et al [12] evaluated the setup uncertainties and anatomical changes in 6 patients with oropharyngeal or oral cavity cancers by using weekly CBCTs to generate sCTs. Their findings showed that for patients with weight-loss of 6% or less, RO-IMPT plans were robust to uncertainties.

While some previous studies used sCTs for HN proton ART, most of these studies had small sample sizes and only 1 reported on the dose accumulation using RO-IMPT for HN tumors located in the inferior portion of the neck (tonsil, base of tongue, larynx, and parotid). In this work we evaluated a larger patient cohort to assess the differences between RO-IMPT planned and delivered doses by performing weekly sCT-based dose accumulation for lower neck tumors. For 2 patients with significant weight loss, daily CBCTs were used to assess if weekly CBCTs were representative of the daily changes. The scans captured setup variations and continuing anatomical changes for such patients. In addition, we provide assessment of the practicality and feasibility of replacing repeat CT scans with sCTs for adaptive IMPT for treatment of HN cancer tumors.

Table 1. Patient characteristics.

Patient identifier	Tumor site	Age	Gender	TNM stage	Dose levels (Gy)
1	Left buccal mucosa	56	M	pT3M0N0	60, 54
2	Left tongue base	56	F	T2N2bM0	70, 60, 54
3	Right tonsil	65	F	pT1N2aM0	66, 60, 54
4	Inferior pole of the left tonsil and adjacent left tongue base	65	M	T1N1M0	60, 54
5	Right anterior floor of the mouth	56	M	pT4apN0M0	60, 56
6	Left tonsil	72	M	cT2N2bM0	70, 60, 54
7	Right tonsil and post-cricoid hypopharynx	62	M	T3N0M0 tonsil & T2N0M0 hypopharynx	70, 60, 54
8	Right tonsil	59	M	cT1N3M0	70, 56
9	Left tonsil	52	M	T1N2aM0	60, 54
10	Right parotid	36	F	pT1N1M0	66, 56
11	Right tongue base	41	F	T3N1	70, 60, 54
12	Right tongue base	67	M	T2N2cM0	70, 60, 54
13	Left pyriform sinus	35	M	pT3N0M0	70, 60, 54
14	Left tonsil	58	M	cT2N1M0	70, 63, 56
15	Right tonsil	71	M	cT2N0M0	70, 66, 60, 54
16	Left tonsil	56	F	T2N1M0	70, 63, 56
17	Left aryepiglottic fold and left vocal cord	66	F	T3 N0 M0	70, 63, 56
18	Larynx	71	M	cT1N0M0	66
19	Left tonsil	44	F	T1N3M0	70, 63, 56
20	Left tonsil	59	M	cT2N1cM0	70, 59.5, 56
21	Left tonsil	49	M	cT2N2M0	70, 60, 56

Abbreviations: TNM, tumor, node, metastases; M, male; F, female.

Materials and Methods

Clinical Data

Twenty-one patients with HN cancer previously treated with volumetric modulated arc therapy using simultaneous integrated boost technique and enrolled in a retrospective institutional review board protocol were included in this study. For all patients, a contrast pCT and a noncontrast pCT were acquired with the patient in a supine position with 1.5-mm slice thickness. All pCT scans were taken with a Siemens Somatom 16 slice CT simulator (Siemens, Forchheim, Germany). Daily CBCT scans for patient setup were acquired with a Truebeam on-board CBCT imager (Varian Medical Systems, Inc, Palo Alto, California) and reconstructed using an iterative CBCT (iCBCT) algorithm [13]. The pCT included all gross target volumes, clinical target volumes (CTVs), planning target volumes, and OARs, including, spinal cord, brainstem, parotids, carotids, constrictors, and larynx. All relevant targets and normal tissues were delineated by the same expert HN radiation oncologist on the contrasted computed tomography (CT) scan, and, subsequently, all contours were transferred to the noncontrast scan via rigid registration for proton planning. **Table 1** shows the characteristics of the patients included in this study. The location of CTVs was in the mid/lower neck area for a vast majority of patients in this study.

IMPT Planning

For each patient, a proton multifield optimization plan was created with an arrangement of 2 or 3 fields depending on target extent and anatomy; for each field, a field-specific target was created encompassing all CTVs. These field-specific targets were then modified to avoid the beam entering through the chin area and going through teeth. Any artifact caused by dental implants was delineated and overridden to an appropriate HU value. The nonlinear universal proton optimizer (NUPO 15.6, Eclipse, Varian) was used for optimization along with a proton convolution superposition algorithm (PCS 15.6, Eclipse, Varian) for dose calculation. The relative biological effectiveness of 1.1 was used for the weighted dose. **Table 2** lists the target dose objectives and OAR constraints used for IMPT planning.

During RO-IMPT, the targets were the only structures that were selected to be robustly optimized with the objective to cover the 95% of each CTV volume with 100% of the prescription dose. For each patient, the ±3-mm setup uncertainties (in cardinal

Table 2. Dose constraints for CTVs and OARs for the nominal IMPT plan.

Parameter	Value
Target	
CTV_54 (N = 12)	D95 > 54 Gy
CTV_56 (N = 8)	D95 > 56 Gy
CTV_60 (N = 14)	D95 > 60 Gy
CTV_63 (N = 4)	D95 > 63 Gy
CTV_66 (N = 4)	D95 > 66 Gy
CTV_70 (N = 14)	D95 > 70 Gy
OAR	
Brainstem	$D_{max} < 54$ Gy
Left cochlea	$D_{mean} < 40$ Gy
Right cochlea	$D_{mean} < 40$ Gy
Constrictors	$D_{mean} < 50$ Gy
Larynx	$D_{mean} < 50$ Gy
Mandible	$D_{max} < 75$ Gy
Oral cavity	$D_{mean} < 50$ Gy
Spinal cord	$D_{max} < 48$ Gy
Left parotid	$D_{mean} < 26$ Gy
Left parotid	V20Gy < 50%
Right parotid	$D_{mean} < 26$ Gy
Right parotid	V20Gy < 50%

Abbreviations: IMPT, intensity modulated proton therapy; CTV, clinical target volume; OAR, organ at risk; D95, relative target volume receiving equal or more than the prescription dose; D_{max}, maximum relative dose delivered to the structure; D_{mean}, mean dose to the volume; V20Gy relative volume of the structure receiving more than 20 Gy.

directions), along with $\pm 3\%$ proton range uncertainties, resulting in 12 uncertainty scenarios, were used during RO. The worst-case scenario was required to achieve V95 > 95% (95% of the volume receiving more than 95% of the prescription dose) for CTV while keeping the normal tissue constraints as low as possible. The full width at half maximum spot size in air was set to 0.425 cm during the optimization process.

Creation of sCT and Dose Accumulation

The sCTs were created by deforming the initial pCT to iCBCTs by using the multi-pass corrected deformable image registration (DIR) algorithm available in the Velocity software package (version 4.1, Varian), which is based on the Mattes formulation of mutual information [13]. The rigid shifts from patient setup were applied before the DIR between pCT and each iCBCT. The DIR was then used to create an sCT by transferring the electron density from pCT to iCBCT frame of reference, and in regions outside the iCBCT FOV these areas were filled with the corresponding image data from the pCT. In addition to the visual assessment of deformations, the anatomical landmarks (eg, bones, air cavities, spinal cord) were visually tracked between pCT and sCBCT to ensure that they matched well. The DIRs were redone by readjusting the region of interest for DIRs that did not pass the quality assurance process [14]. At this stage we decided to exclude 8 CTV_tertiary (CTV$_3$) targets due to the small FOV of the iCBCT, since these areas in the shoulder demonstrated poor DIR performance. The sCTs were then sent back to the treatment planning system so the dose could be recalculated on each sCT. After dose recalculation, these doses were sent back to adaptive workflow in Velocity for dose accumulation. The weekly dose accumulations were performed every 5 fractions, that is, once per week.

Delivered Versus Planning Dose

For each patient, weekly dose accumulation from the RO-IMPT plan was evaluated and compared using the dosimetric indexes listed in **Table 2** for the nominal plan. The difference between dose volume indexes were performed by 2-sided Wilcoxon signed-rank test. A *P* value <.05 indicates the significant difference. Daily accumulation for 2 patients with moderate and large weight loss (patient 14 and patient 21) were compared with weekly accumulation using the dosimetric indexes in

Table 3. Planned and weekly accumulated dose-volume indexes averaged over all patients.

|	Plan	Accumulation	Difference	*P* value
D_{max} (%)	111.41 ± 4.07	110.16 ± 3.24	−1.25 ± 1.98	.005
Brainstem D_{max} < 54 Gy	22.89 ± 9.92	22.70 ± 9.29	−0.19 ± 1.90	.722
Left cochlea D_{mean} < 40 Gy	7.85 ± 8.49	8.57 ± 9.54	0.72 ± 1.65	.198
Right cochlea D_{mean} < 40 Gy	7.23 ± 8.57	7.46 ± 8.29	0.24 ± 1.13	.146
Constrictors D_{mean} < 50 Gy	43.68 ± 14.34	43.28 ± 14.65	−0.41 ± 0.83	.099
Larynx D_{mean} < 50 Gy	33.94 ± 15.76	34.12 ± 15.89	0.18 ± 1.48	.353
Mandible D_{max} < 75 Gy	64.79 ± 14.73	64.72 ± 15.05	−0.07 ± 2.66	.725
Oral cavity D_{mean} < 50 Gy	20.55 ± 12.54	21.59 ± 13.45	1.05 ± 1.51	.004
Spinal cord D_{max} < 48 Gy	34.18 ± 12.43	33.22 ± 11.59	−0.80 ± 2.57	0.202
Left parotid D_{mean} < 26 Gy	20.44 ± 10.30	21.95 ± 10.45	1.50 ± 2.19	<.001
Left parotid V20Gy < 50%	42.46 ± 22.88	45.66 ± 23.22	3.20 ± 5.02	.002
Right parotid D_{mean} < 26 Gy	17.46 ± 13.07	19.08 ± 13.25	1.62 ± 2.03	<.001
Right parotid V20Gy < 50%	35.63 ± 26.25	38.99 ± 26.49	3.36 ± 4.61	.004
CTV primary V95 (%) (N = 21)	99.65 ± 0.41	98.16 ± 1.35	−1.49 ± 1.34	<.001
CTV secondary V95 (%) (N = 18)	99.58 ± 0.51	98.08 ± 1.74	−1.50 ± 1.47	<.001
CTV tertiary V95 (%) (N = 9)	99.33 ± 0.59	96.58 ± 3.01	−2.75 ± 3.02	.004

Abbreviations: D_{max}, maximum dose in percentage calculated for the body; D_{mean}, mean dose to the volume; V20Gy relative volume of the structure receiving more than 20 Gy; CTV, clinical target volume; V95, 95% of the volume receiving a given percentage of the prescription dose.

Table 2 and applying gamma index using 2%/2 mm criteria with a 10% dose threshold between the dose distributions (daily and weekly).

Results

Table 3 shows the differences between the nominal plan and accumulated dose-volume indexes averaged over all patients. Statistically significant differences were observed for the maximum body dose, both parotids, and all CTVs. The accumulated dose V95 for the CTV_primary (CTV$_1$) was 98.34% ± 1.38%, which was −1.32% ± 1.42% (*P* < .001) lower volume coverage than the nominal plan. Differences for CTV_secondary (CTV$_2$) and CTV$_3$ corresponded to −1.50% ± 1.47% (*P* < .001) and −2.75% ± 3.02% (*P* < .004). The difference between the nominal and accumulated plan maximum dose (D_{max}) was −1.25% ± 1.98% (*P* < .005). The right and left parotid mean dose (D_{mean}) resulted in an average difference of 1.62 ± 2.03 cGy and 1.50 ± 2.19 cGy, respectively, between the accumulated and nominal IMPT plans (*P* < .001); 3 patients had an accumulated dose higher than the nominal plan and violated the D_{mean} < 26 Gy for the left parotid, and 2 patients for the right parotid. The difference between nominal and accumulated D_{mean} for the oral cavity was 1.05 ± 1.51 cGy (*P* < .004). The remaining OARs did not show statistically significant deviations between the nominal and accumulated plans. **Figure 1** shows the number of weekly sCT-based calculated doses that passed (above the line and green) or failed (below the line and red) the 95% CTV coverage for the 3 CTVs. Of the 21 patients, 9 had weekly doses of CTV$_1$ below V95, from which a total of 17 weekly doses corresponded to undercoverage, and 12 of these were lower than the RO-IMPT worst-case scenario. One patient, patient 12, had an accumulated dose just below V95, with more than half of the weekly sCTs below coverage with a range of 78.83% through 98.02%. For CTV$_2$, 6 patients had weekly sCTs below V95; 5 of these patients were the same as those with undercoverage of CTV$_1$. Consistently, patient 12 had CTV$_2$ weekly doses below V95, and the accumulated dose was lower than the RO worst-case scenario. Eight of the patients had a CTV$_3$, and 6 of these had weekly doses below V95. Patient 3 had an accumulated dose lower than the RO worst-case scenario, and 6 of the 7 weekly doses violated the V95 > 95%.

The weekly sCT doses for the OARs that were significantly different (parotids and oral cavity) compared with the nominal plan are shown in **Figure 2**. The nominal plan D_{mean}, the total accumulated D_{mean}, and the RO-IMPT worst-case scenario D_{mean} are also shown in the same plot. For the left parotid all patients, except 2 (patient 13 and patient 15) had an accumulated D_{mean} lower than the worst-case scenario. Patient 13 was the only patient who violated the worst-case scenario and had an accumulated dose higher than the D_{mean} < 26Gy constraint. The remaining 8 patients with D_{mean} > 26Gy had RO-IMPT plans that also violated the constraint. For the right parotid, patient 14 and patient 17 had accumulated D_{mean} higher than the worst-case scenario plan but did not violate the D_{mean} < 26 Gy constraint. The oral cavity and constrictors accumulated dose were all lower than those predicted by the worst-case scenario.
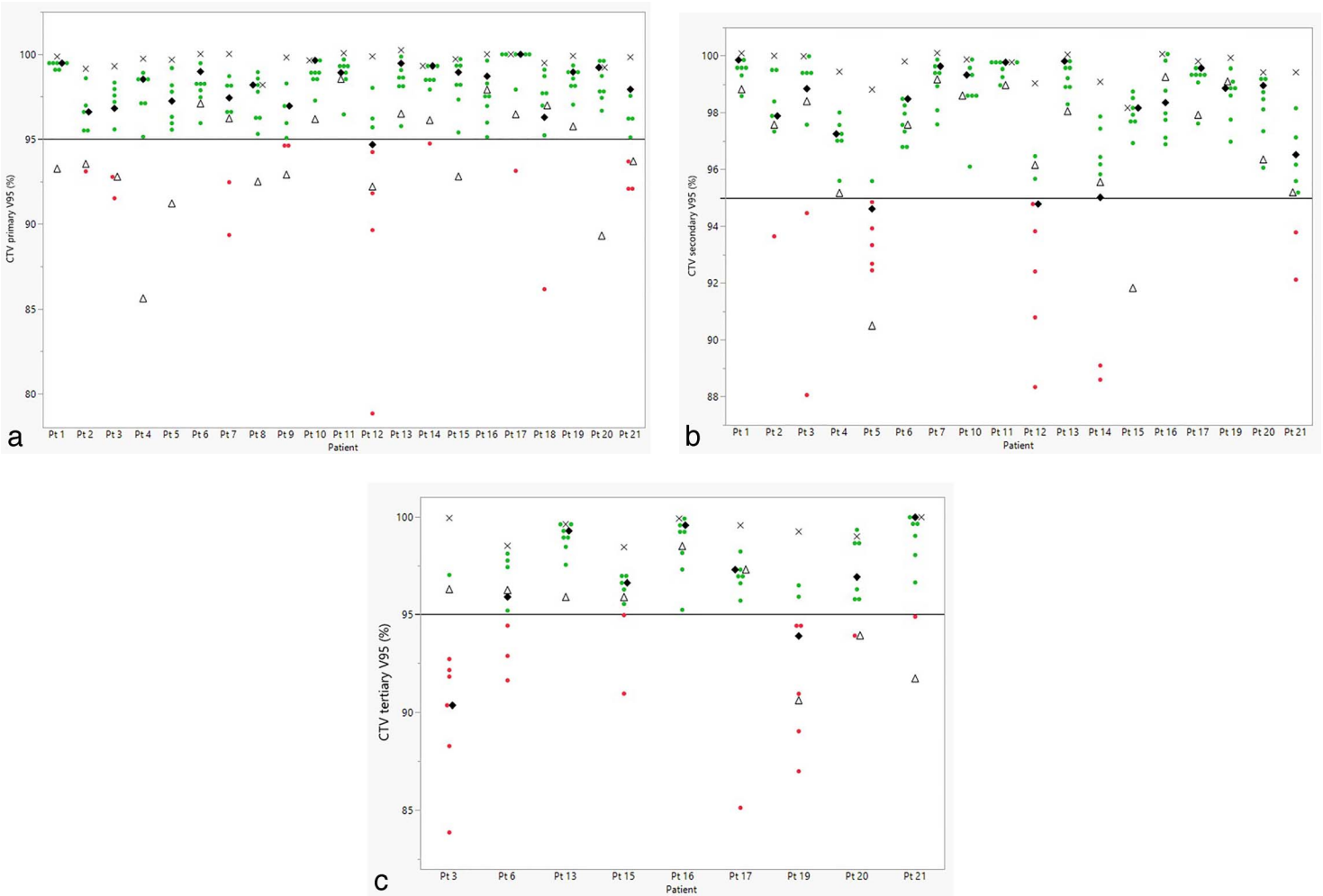
Figure 1. Scatter plot of CTV coverage (V95) for each patient for the weekly sCT dose. Panel (a) illustrates CTV_1, (b) CTV_2, and (c) CTV_3. The colored dots represent the weekly dose calculated from the sCT; values under the solid line failed the 95% dose coverage constraint. The "x" symbol represents the nominal plan dose, the solid diamond represents the accumulated dose for the treatment course, and the triangle is the worst-case scenario from RO-IMPT. Abbreviations: CTV, clinical target volume; V95, 95% of the volume receiving a given percentage of the prescription dose; CTV_1, CTV_primary; (b) CTV_2 . CTV_secondary; CTV_3, CTV_tertiary; sCT, synthetic computed tomography; RO-IMPT, robust optimization intensity modulated proton therapy.

Robust evaluation of the weekly doses resulted in 88.7% of the fractions for the left parotid and 83.7% for the right parotid, being lower than the worst-case scenario. For the oral cavity and constrictors the percentage of fractions that were better than the worst-case were of 91.1% and 97.0%, respectively. The coverage of the targets in the weekly sCTs within the robustness bands were 84.5%, 68.0%, and 60.3% for the CTV_1, CTV_2, and CTV_3, respectively.

The DVHs of a patient who experienced mild weight loss leading to small changes in anatomy is shown in **Figure 3**. Panel a displays the doses for the 3 CTV dose levels, constrictors, oral cavity, brainstem, and spinal cord; the solid line on the left graph is the nominal plan DVH, and the dotted line is the accumulated DVH along with the robust evaluation bands of ± 3 mm/ $\pm 3\%$ uncertainties and on the right are the weekly DVHs. On panel b, the left and right parotids are displayed separately for clarity. The accumulated DVHs for all the structures fell within the uncertainty bands, yet the weekly DVHs show more variation with a few curves surpassing the bands.

An example of a patient (patient 14) who had significant weight loss is illustrated in **Figure 4**. Results showed considerable deviation of the accumulated plan compared with the nominal plan for the parotids and mandible, falling outside of the ± 3 mm/ $\pm 3\%$ robust evaluation bands. The CTV_1 coverage remained within the uncertainty bands, but the coverage to the CTV_2 deviated in 3 out of the 7 weekly calculations. The oral cavity accumulated D_{mean} fell at the border of the worst-case scenario, but 4 of the 7 weekly dose calculations showed higher than expected doses.
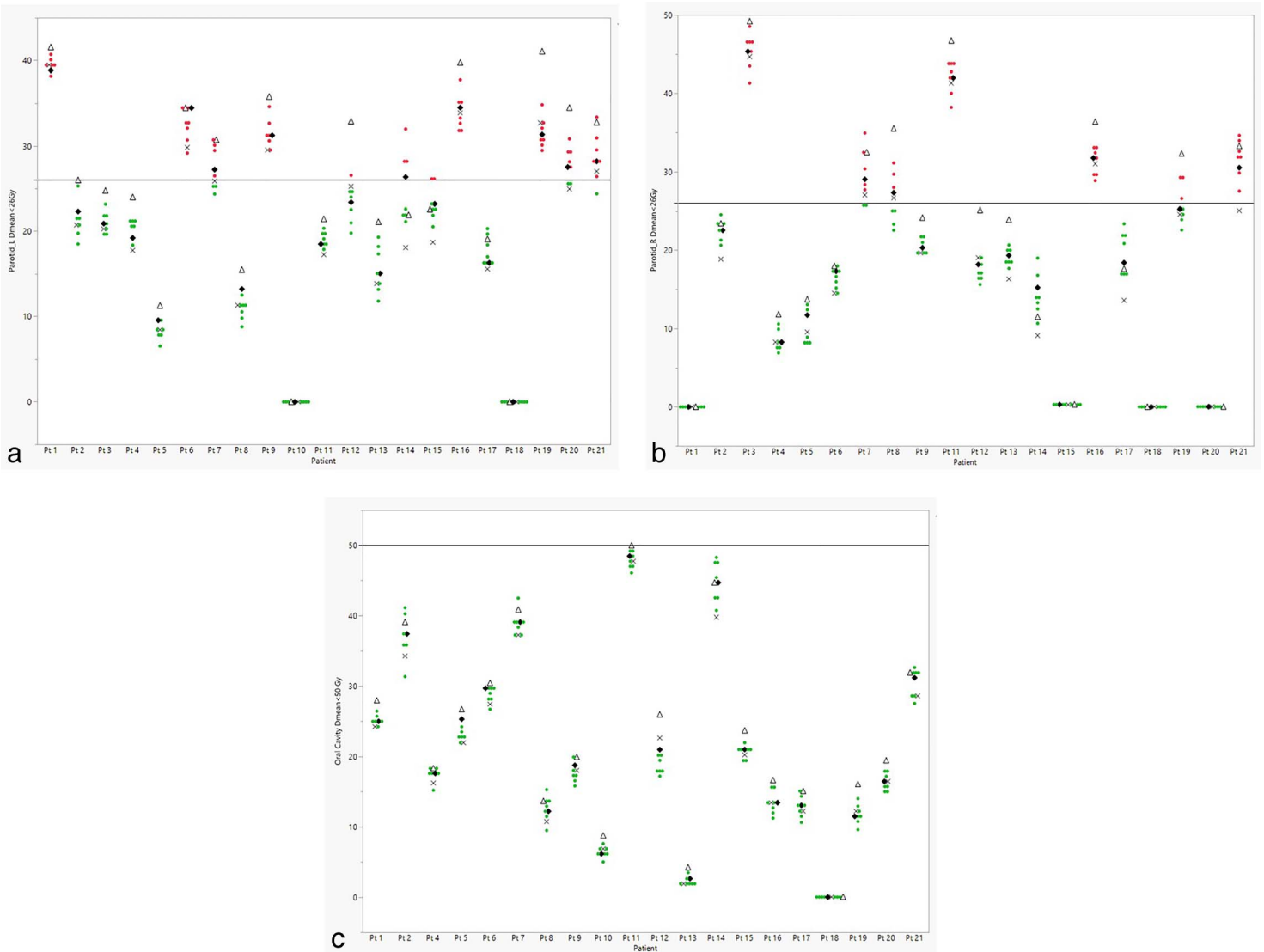
Figure 2. Scatter plot of the nominal plan, accumulated dose, and weekly D_{mean} to the left parotid (a), right parotid (b), and oral cavity (c) for each patient. The colored dots represent the weekly dose calculated from the sCT, values over the solid line represent doses above OAR constraint. The "x" symbol represents the nominal plan dose, the solid diamond represents the accumulated dose for the treatment course, and the triangle is the worst-case scenario from RO-IMPT. Abbreviations: D_{mean}, mean dose; OAR, organs at risk; sCT, synthetic computed tomography; RO-IMPT, robust optimization intensity modulated proton therapy.

The isodose distribution for the same patient with extreme weight loss (patient 14) is displayed in **Figure** 5, where the axial dose distribution of the left panel is the nominal plan, the middle panel is the accumulated dose distribution on the same axial slice, and the right panel is the nominal dose distribution subtracted from the accumulated dose distribution. It is well illustrated how the parotids and oral cavity were overdosed due to the change in anatomy while the target was underdosed. This is a good example of an extreme case displaying how anatomy can change during the course of radiotherapy.

The daily dose accumulations for patient 14 and patient 21 were compared with the weekly dose accumulation and shown in **Table 4**. The gamma analysis showed that both dose distributions were comparable, with more than 95% meeting the criteria. The differences between the daily and weekly dose indexes were less than 4.4%. **Figure 6** shows the DVHs for the nominal, weekly and daily accumulation dose distributions. Panel a shows the DVHs for patient 14 with the parotids displayed in a separate graph, panel b shows the same for patient 21 with left and right parotids shown in separate graphs, and panel c illustrates the dose difference between daily and weekly dose accumulations.
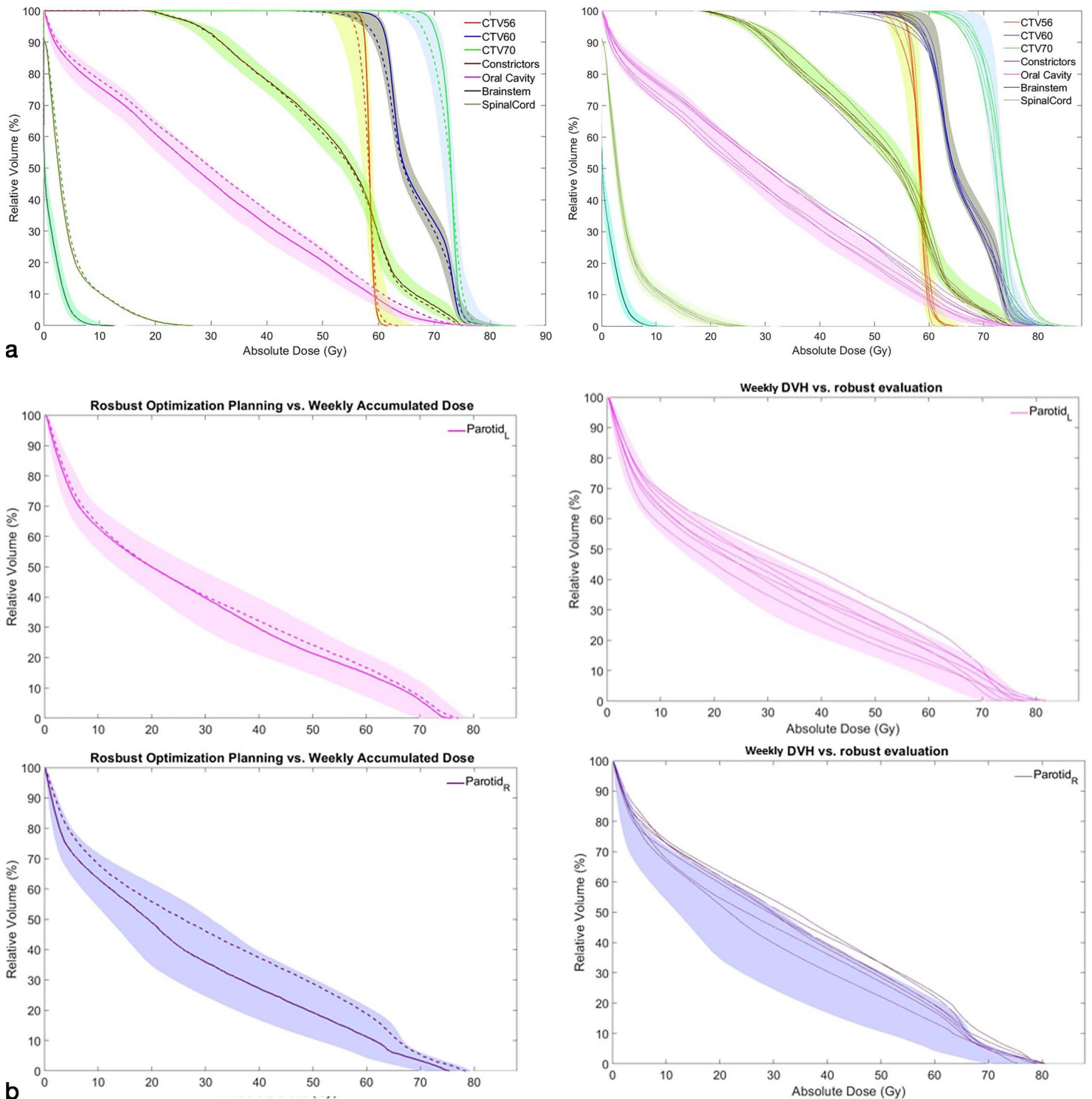
Figure 3. DVH comparisons for a single patient (patient 21) with mild weight loss. (a) CTVs, constrictor, mandible, and oral cavity and (b) left and right parotid. The planned dose (solid line) and accumulated dose (dashed line) are shown on the left graph of each panel, and the shaded region represents the original plan range of uncertainty scenarios. The graphs on the right show the weekly DVHs along with the uncertainly bands from RO-IMPT. Abbreviations: CTV, clinical target volume; DVH, dose volume histogram; RO-IMPT, robust optimization intensity modulated proton therapy.
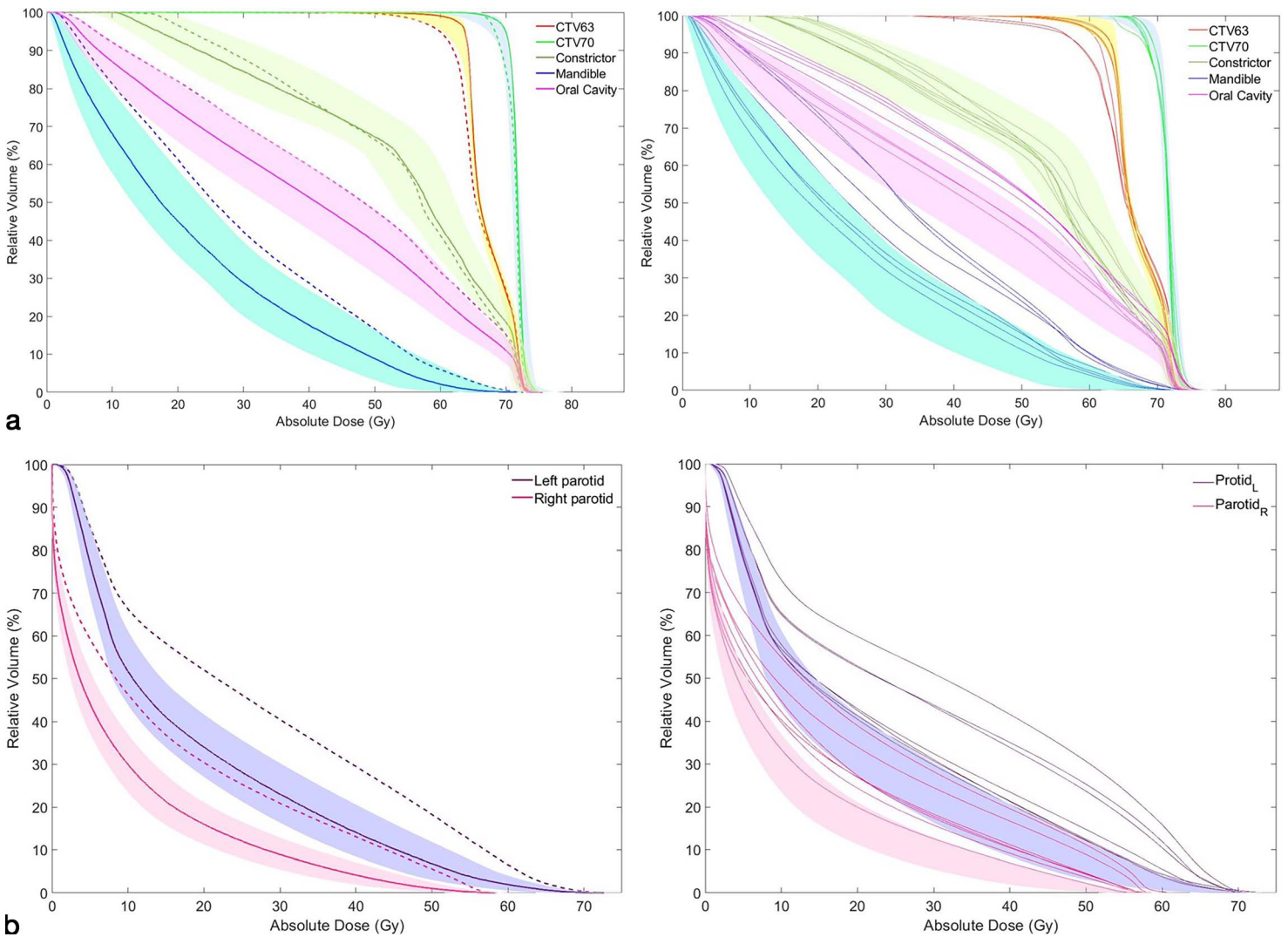
Figure 4. DVH comparisons for a single patient (patient 14) with significant weight loss. (a) CTVs, constrictor, mandible and oral cavity and (b) left and right parotid. The planned dose (solid line) and accumulated dose (dashed line) are shown on the left graph of each panel and the shaded region represent the original plan range of uncertainty scenarios. The graphs on the right show the weekly DVHs along with the uncertainly bands. Abbreviations: CTV, clinical target volume; DVH, dose volume histogram.

Discussion

It is well understood that protons are more susceptible to setup and anatomical uncertainties, in addition to the inherent range uncertainty, and complex and heterogeneous anatomy, such as HN, are even more susceptible. In this study, we assessed the dosimetric differences between planned and accumulated weekly doses using sCTs for RO plans generated with ±3 mm/ ±3% uncertainty scenarios for HN cancer patients with lower neck tumors treated with simultaneous integrated boost technique.

To ensure that the weekly CBCTs were representative of the daily setup and anatomical changes, dose accumulation from the daily CBCTs for the 2 patients with the largest weight loss were compared with the dose accumulation from the weekly CBCTs. These results show that weekly dose accumulation can be representative of the daily changes.

We found that for the CTV_1, the weekly accumulated dose exhibited a V95 of 98.16% ±1.35%, while the coverage was 99.65% ± 0.41% on the nominal plan. Similarly, the accumulated V95 for the CTV_2 was 98.08% ± 1.74% compared with 99.58% ± 0.51% in the nominal plan. While the CTV_3 seemed to remain well covered, similarly to Landry et al [10], we found that the DIR did not perform well beyond the limit of the CBCT FOV in the shoulder area, where the algorithm used the pCT to complete the sCT. Therefore, we cannot determine the accumulated dose for all tertiary CTVs with confidence. Those patients

a. Nominal Planned Dose | b. Accumulated dose | c. Difference between a and b
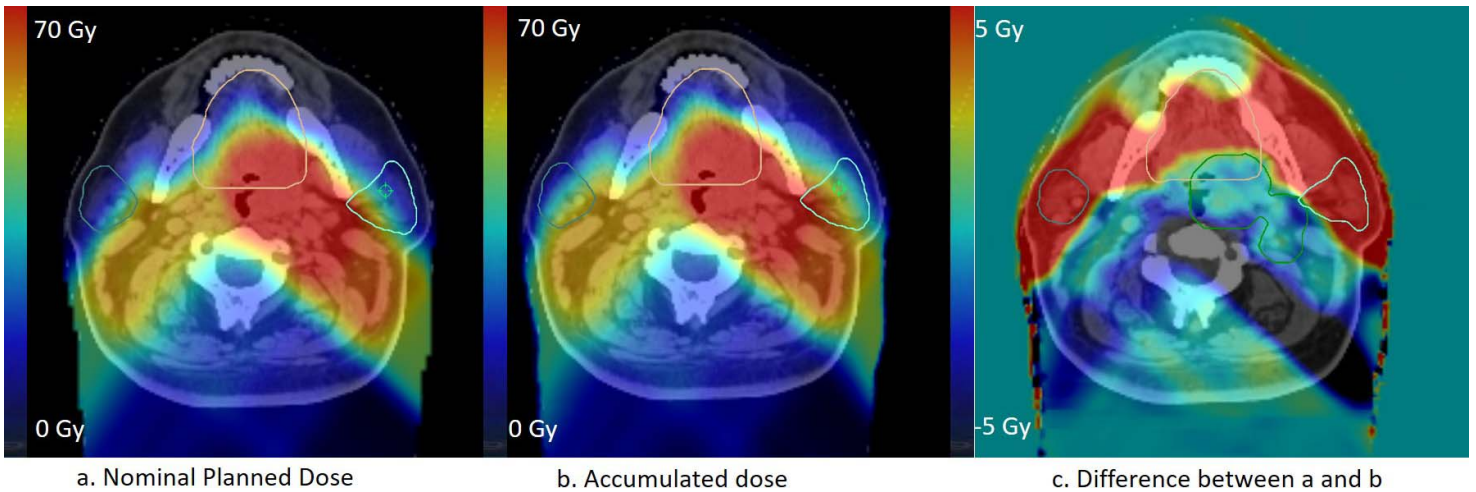
Figure 5. Dose difference map (c) between the nominal planning dose (a) and the weekly accumulated dose (b) for patient 14, who had significant weight loss. In panel (c), areas of positive dose represent accumulated doses greater than the nominal plan, and vice versa.

in whom the sCTs were not adequate in these areas were excluded from the analysis. To include these areas, a large CBCT FOV would be necessary, which would degrade the image resolution. Another method is to stitch 2 CBCTs acquired sequentially and then combine them to cover the full treatment area [10, 15].

Kraan et al [16] analyzed the effects of treatment uncertainties on delivered dose using simulated individual and combined errors (setup, anatomy, and range) and the effects of replanning for 10 patients with oropharyngeal cancer. This study, which used a pCT and only 1 rCT during the course of radiotherapy, showed that individual errors did not lead to serious target underdosage (D98% > 95%) but combined effects of errors did. They reported that the percentages of simulations for CTV_1 and CTV_2 satisfying the D98% > 95% for combined errors were 69% and 88%, respectively. By applying adaptive planning,

Table 4. Daily and weekly accumulated dose-volume indexes and gamma analysis for patient 14 and patient 21.

	Patient 14			Patient 21		
	Plan	Weekly accumulation	Daily accumulation	Plan	Weekly accumulation	Daily accumulation
D_{max} (%)	107.81	107.94	107.21	120.84	114.74	113.96
Brainstem D_{max} < 54 Gy	15.66	14.49	15.19	12.64	12.63	12.51
Left cochlea D_{mean} < 40 Gy	6.95	6.93	6.88	6.04	6.05	6.09
Right cochlea D_{mean} < 40 Gy	0.00	0.00	0.00	10.93	10.93	10.88
Constrictors D_{mean} < 50 Gy	52.80	53.16	53.47	51.68	51.36	51.27
Larynx D_{mean} < 50 Gy	39.37	40.33	40.90	37.75	38.13	38.21
Mandible D_{max} < 75 Gy	71.68	72.66	72.05	80.25	73.45	75.23
Oral cavity D_{mean} < 50 Gy	39.76	44.58	44.27	28.94	31.17	31.69
Spinal cord D_{max} < 48 Gy	40.02	34.97	35.61	26.71	26.55	26.34
Left parotid D_{mean} < 26 Gy	18.09	26.35	26.34	26.80	27.92	29.20
Left parotid V20Gy < 50%	34.03	51.93	51.64	49.94	49.86	50.89
Right parotid D_{mean} < 26 Gy	9.09	15.22	15.01	25.06	30.51	30.32
Right parotid V20Gy < 50%	15.99	30.35	30.09	48.83	55.68	55.01
CTV primary V95 (%)	99.34	99.20	99.45	99.81	97.62	97.29
CTV seconary$_2$V95 (%)	99.09	95.02	94.57	99.43	96.52	96.73
CTV tertiary V95 (%)				99.98	99.79	99.28
Gamma index (2%/2 mm) (%)		95.97			98.12	

Abbreviations: D_{max}, maximum dose in percentage calculated for the body; D_{mean}, mean dose to the volume; V20Gy relative volume of the structure receiving more than 20 Gy; CTV, clinical target volume; V95, 95% of the volume receiving a given percentage of the prescription dose.

gamma index dose comparison between daily and weekly dose distributions utilizing 2%/2mm criteria

Figure 6. Daily vs weekly DVH comparisons for patient 14 (a) and patient 21 (b). The solid line is the planned dose, the dashed line is the weekly dose accumulation, and the dotted line is the daily dose accumulation. In each panel (a and b) the graphs are separated for clarity. Panel (c) illustrates the daily and weekly dose accumulation differences for patient 14 (left) and patient 21 (right). The contour shown corresponds to the CTV_1 for reference. Abbreviations: CTV_1, clinical target volume primary; DVH, dose volume histogram.
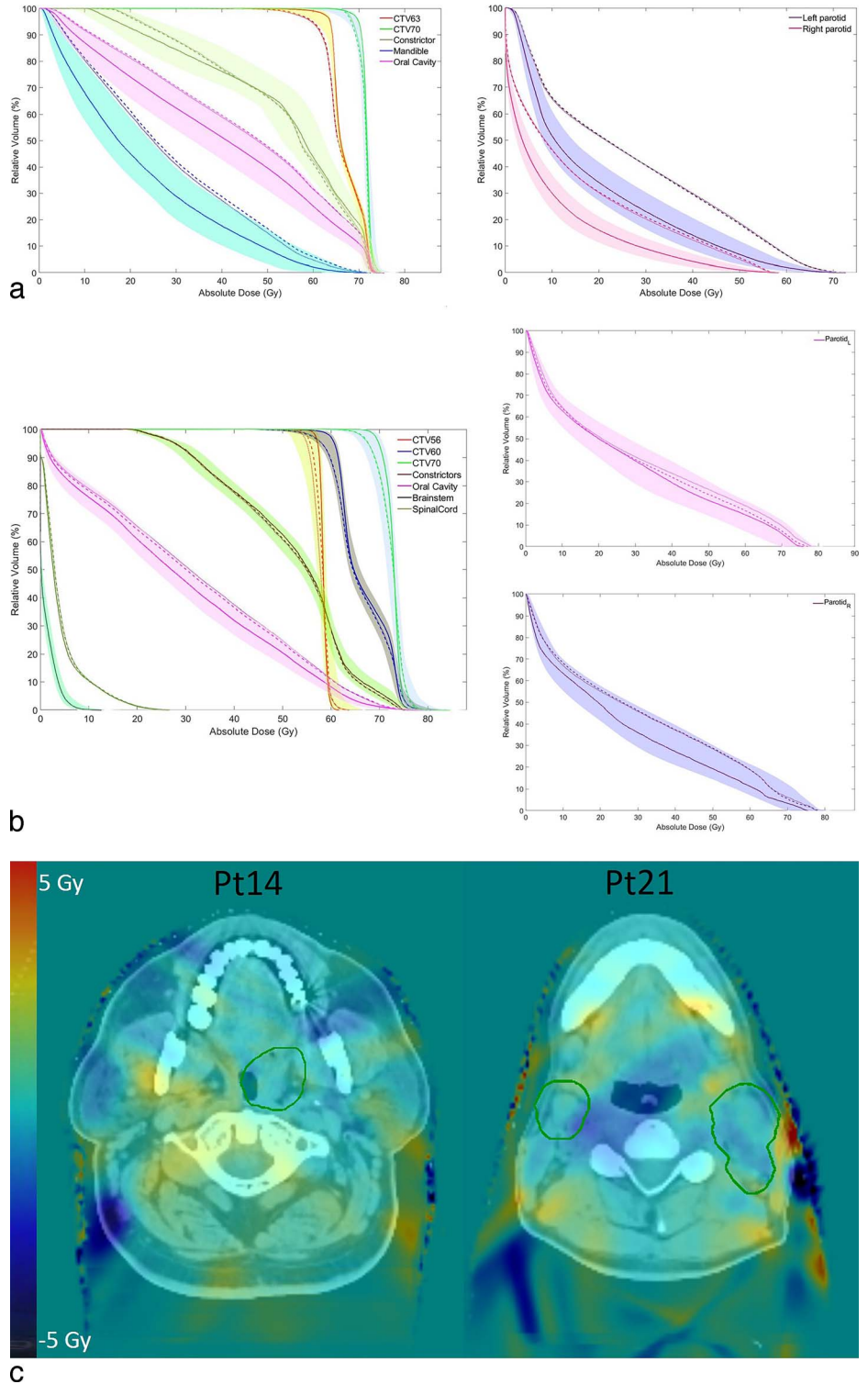
the target coverage showed an increase to 96% and 100% corresponding to CTV_1 and CTV_2. Compared with our results using RO-IMPT, 84.5% of patients satisfied the D95% > 95% worst-case scenario for CTV_1 and 68.0% for CTV_2.

For HN proton therapy, verification CTs are imperative, but these CTs increase the workload, which can strain departmental resources [17]. In this study, we focused on treatment sites in the lower neck and demonstrated that using an sCT to track anatomical changes along with dose distribution can be used in lieu of an rCT. Kurz et al [9] also used sCTs to evaluate plan adaptation and compared it to an rCT adapted plan for hypopharyngeal and nasopharyngeal areas. Their work exhibited small

differences between these 2 CT data sets (sCT and rCT), and these differences may have resulted from different times of acquisition and the resulting DIR contours. They suggested that the use of RO might mitigate the large dosimetric changes in an rCT or sCT. This was one of the motivations for our current study: to determine if RO could accommodate the bulk of these anatomical and setup uncertainties, or whether adaptive replanning was necessary to account for these changes. The findings presented here showed that, for the bulk of the changes experienced through the treatment course, RO does properly accommodate these changes; however, for cases in which the changes are quite significant, plan adaptation is required. This indicates that monitoring patients throughout the treatment course is necessary to determine if these changes require plan adaptation.

The workflow for creating the sCTs from CBCT in the patient's daily treatment position can be used easily to replace rCTs for verification during the treatment course. The sCT can be used for DVH and isodose distribution evaluation to determine the need for treatment adaptation. The procedure is automated, with some human interaction to assess DIR and contour propagation. In the future, using sCTs for direct plan adaptation would result in a significant time and resource savings for patients and radiation oncology staff.

Conclusions

In this study, we generated sCTs by deforming the on-board CBCT and using the pCT electron density information to generate weekly dose distributions for HN patients. In addition, we calculated the accumulated dose and compared this with the RO-IMPT worst-case scenario values. The dose coverage of V95 > 95% for the primary CTV was met for most patients, demonstrating that RO-IMPT accommodates for most setup and anatomical changes observed. OAR doses were lower than the RO-IMPT worst-case scenario in most instances. We therefore showed that RO-IMPT helps with anatomical and setup uncertainties and further demonstrated that use of sCT can be a tool to evaluate the need for treatment adaptation.

ADDITIONAL INFORMATION AND DECLARATIONS

References

1. van de Water TA, Lomax AJ, Bijl HP, de Jong ME, Schilstra C, Hug EB, Langendijk JA. Potential benefits of scanned intensity-modulated proton therapy versus advanced photon therapy with regard to sparing of the salivary glands in oropharyngeal cancer. *Int J Radiat Oncol Biol Phys*. 2011;79:1216–24.

2. Lomax AJ. Intensity modulated proton therapy and its sensitivity to treatment uncertainties 1: the potential effects of calculational uncertainties. *Phys Med Biol*. 2008;53:1027–42.

3. Lomax AJ. Intensity modulated proton therapy and its sensitivity to treatment uncertainties 2: the potential effects of inter-fraction and inter-field motions. *Phys Medi Biol*. 2008;53:1043–56.

4. Liu W, Frank SJ, Li X, Li Y, Park PC, Dong L, Ronald Zhu X, Mohan R. Effectiveness of robust optimization in intensity-modulated proton therapy planning for head and neck cancers. *Med Phys*. 2013;40:051711.

5. Wu QJ, Li T, Wu Q, Yin F-F. Adaptive radiation therapy: technical components and clinical applications. *Cancer J*. 2011;17: 182–9.

6. Park Y-K, Sharp GC, Phillips J, Winey BA. Proton dose calculation on scatter-corrected CBCT image: feasibility study for adaptive proton therapy. *Med Phys*. 2015;42:10.

7. Kim J, Park Y-K, Sharp G, Busse P, Winey B. Water equivalent path length calculations using scatter-corrected head and neck CBCT images to evaluate patients for adaptive proton therapy. *Phys Medicine Biol*. 2017;62:59–72.

8. Kurz C, Kamp F, Park YK, Zöllner C, Rit S, Hansen D, Podesta M, Sharp GC, Li M, Reiner M, Hofmaier J, Neppl S, Thieke C, Nijhuis R, Ganswindt U, Belka C, Winey BA, Parodi K, Landry G. Investigating deformable image registration and scatter correction for CBCT-based dose calculation in adaptive IMPT. *Med Phys*. 2016;43:5635.

9. Kurz C, Nijhuis R, Reiner M, Ganswindt U, Thieke C, Belka C, Parodi K, Landry G. Feasibility of automated proton therapy plan adaptation for head and neck tumors using cone beam CT images. *Radiat Oncol*. 2016;11:64.

10. Landry G, Nijhuis R, Dedes G, Handrack J, Thieke C, Janssens G, Orban de Xivry J, Reiner M, Kamp F, Wilkens JJ, Paganelli C, Riboldi M, Baroni G, Ganswindt U, Belka C, Parodi K. Investigating CT to CBCT image registration for head and neck proton therapy as a tool for daily dose recalculation. *Med Phys*. 2015;42:1354–66.

11. van de Water S, Albertini F, Weber DC, Heijmen BJM, Hoogeman MS, Lomax AJ. Anatomical robust optimization to account for nasal cavity filling variation during intensity-modulated proton therapy: a comparison with conventional and adaptive planning strategies. *Phys Med Biol*. 2018;63:025020.

12. Hague C, Aznar M, Dong L, Fotouhi-Ghiam A, Lee LW, Li T, Lin A, Lowe M, Lukens JN, McPartlin A, O'Reilly S, Slevin N, Swisher-Mcclure S, Thomson D, Herk MV, West C, Zou W, Teo B-KK. Inter-fraction robustness of intensity-modulated proton therapy in the post-operative treatment of oropharyngeal and oral cavity squamous cell carcinomas. *Br J Radiol*. 2020;93:20190638.

13. Kadoya N, Fujita Y, Katsuta Y, Dobashi S, Takeda K, Kishi K, Kubozono M, Umezawa R, Sugawara T, Matsushita H, Jingu K. Evaluation of various deformable image registration algorithms for thoracic images. *J Radiat Res*. 2014;55:175–82.

14. Lin H, Ayan A, Zhai H, Zhu T, Both S. SU-GG-I-109: a quantitative evaluation of velocity AI deformable image registration. *Med Phys*. 2010;37:3126.

15. Kong VC, Marshall A, Chan HB. Cone beam computed tomography: the challenges and strategies in its application for dose accumulation. *J Med Imaging Radiat Sci*. 2016;47:92–7.

16. Kraan AC, van de Water S, Teguh DN, Al-Mamgani A, Madden T, Kooy HM, Heijmen BJM, Hoogeman MS. Dose uncertainties in IMPT for oropharyngeal cancer in the presence of anatomical, range, and setup errors. *Int J Radiat Oncol Biol Phys*. 2013;87:888–96.

17. Zhang X, et al., Principles of intensity-modulated proton therapy treatment planning, in Proton Therapy, S.J. Frank and X.R. Zhu, Editors. 2021, Elsevier: Philadelphia. p. 56–79.